Published in final edited form as:
Cancer Res. 2009 December 15; 69(24): 9236–9244. doi:10.1158/0008-5472.CAN-09-2067.

Activating Peroxisome Proliferator-activated Receptor γ Mutant Promotes Tumor Growth *in vivo* by Enhancing Angiogenesis

Lifeng Tian[1,*], **Jie Zhou**[1,*], **Mathew C. Casimiro**[1,2], **Bing Liang**[1], **John O. Ojeifo**[4], **Min Wang**[1], **Terry Hyslop**[3], **Chenguang Wang**[1,2], and **Richard G. Pestell**[1,2]

[1] Department of Cancer Biology, Thomas Jefferson University, 233 S. 10th Street, Philadelphia, PA 19107

[2] Kimmel Cancer Center, Thomas Jefferson University, 233 S. 10th Street, Philadelphia, PA 19107

[3] Division of Biostatistics, Thomas Jefferson University, 233 S. 10th Street, Philadelphia, PA 19107

[4] Lombardi Comprehensive Cancer Center, Georgetown University Medical Center, Research Building, 3970 Reservoir Road NW, Washington, DC 20057

Abstract

Peroxisome proliferator activated receptor γ(PPARγ) is expressed in a variety of cancer cells. The addition of ligand activates the receptor by inducing a conformational change in the receptor, which can be recapitulated by mutation. To investigate the role of activated PPARγ signaling in breast cancer, we compared the function of a constitutively active PPARγ (PγCA) mutant with the wild-type PPARγ in ErbB2-induced mammary tumorigenesis *in vivo*. Tumor cells transduced with either PPARγ or PγCA were implanted into immune competent FVB mice. Enhanced tumor growth was observed in PγCA-transduced celsl, which was associated with increased angiogenesis and endothelial stem cells as evidenced by increased number of cells stained with von Willebrand factor (vWF), c-Kit, CD133 and CD31. Genome-wide expression profiling identified a group of genes within the angiogenesis pathway, including Angptl4, as targets of activated PPARγ; PγCA also induced Angptl4 protein secretion in ErbB2-transformed mammary epithelial cells. Angptl4 promoted vascular endothelial cell migration and conversely immuno-depletion of Angptl4 reduced PγCA-mediated cellular migration. Collectively, these studies suggest that activated PPARγ induces Angptl4 to promote tumor growth through enhanced angiogenesis *in vivo*.

Introduction

The peroxisome proliferator-activator receptors are ligand-activated nuclear receptors that include PPARα, PPARγ and PPARδ (1). PPARγ, originally cloned as a transcription factor involved in fat cell differentiation (2), is activated by endogenous ligands, such as fatty acids produced by sterol response element binding protein 1 (SREBP1) and fatty acids synthase (FASN) pathway (3) and synthetic ligands including the thiazolidinediones (TZD). Viral transduction of the murine liver with PPARγ induces hepatic steatosis (4). This differentiation function of PPARγ is antagonized in cultured cells and *in vivo* by endogenous levels of cyclin D1 (5). PPARγ regulates expression of secreted proteins, such as ACRP30 (6), which in turn may affect heterotypic signaling from nearby cells.

Correspondence to: Chenguang Wang, Thomas Jefferson University, Departments of Cancer Biology, Kimmel Cancer Center, Bluemle Building, Rm 1032, 233 South 10th St, Philadelphia, PA, 19107, chenguang.wang@jefferson.edu.

*Equal contribution

It is estimated that at least 2 million patients take anti-diabetic drugs that function as PPARγ ligands. Understanding the role of this receptor, including its possible role in cancer, is therefore important. Independent lines of evidence support a role for PPARγ to either inhibit or promote tumorigenesis. In studies of NMU-induced mammary tumorigenesis in rats, PPARγ ligands prevented tumor initiation (7) and DMBA-induced mammary tumorigenesis was inhibited by a synthetic ligand, troglitazone (8). PPARγ is expressed in breast, prostate, and colonic epithelium and addition of ligands to cultured cancer cell lines derived from these tissues inhibits cellular proliferation (9–13). Heterozygous mutations of PPARγ have been detected in over 80% of patients with colon cancer (14) and chromosomal translocation between PAX8 and PPARγ in follicular thyroid cancer enhanced cellular proliferation (15).

In contrast with these findings, several studies suggest PPARγ activation may enhance tumor growth. PPARγ ligands increased polyp numbers in the Apc^{Min} model of familial adenomatosis (16,17) and PPARγ inhibits β-catenin abundance only in the presence of wild-type APC (17), raising the possibility that the genetic environment of the host may determine the outcome of PPARγ activation. PPARγ ligands may function independently of the PPARγ receptor with growth inhibition demonstrated in cells lacking PPARγ (18–20). In order to determine the role of the PPARγ and avoid the potential spurious effect of receptor-independent functions, a constitutively active PPARγ (PγCA) was generated, which selectively activated a PPARγ response element without regulating other nuclear receptors. When targeted to mammary epithelium, PγCA collaborated in mammary oncogenesis with polyoma middle T antigen (21).

Human breast cancer is associated with ErbB2 amplification or overexpression in >30% of patients. Although PPARγ is reduced in ErbB2 induced tumor, the role of PPARγ in growth control of ErbB2-induced tumorigenesis is poorly understood. Herein, we demonstrated that PPARγ enhanced ErbB2-induced mammary tumorigenesis *in vivo*. PγCA promoted tumor angiogenesis through induction of the pro-angiogenic factor Angptl4. Genome-wide expression profiling identified Angptl4 and Wnt5a as targets of PPARγ. Angptl4 promoted migration of vascular endothelial cells and immuno-depletion of Angptl4 diminished the effect of PγCA in promoting cellular migration. Thus activated PPARγ enhances angiogenesis and tumor growth *in vivo*. As PPARγ-activating ligands are widely used to treat diabetes, a careful further analysis of breast cancer risk may be warranted.

Materials and Methods

Mice

All animal experiments were performed following animal protocols that had been approved by the Institutional Animal Care and Use Committee (IACUC) at Thomas Jefferson University.

Cell Culture

Human embryonic kidney 293T (HEK293T) was maintained in Dulbecco's Modified Eagle's Medium (DMEM) containing penicillin and streptomycin (100 mg of each/liter) and supplemented with 10% fetal bovine serum (FBS) (5). MCF10A and MCF10A transformed with oncogene NeuT (MCF10A/NeuT) were cultured in DMEM/F12 (50:50) supplemented with 5% horse serum, 5% FBS, insulin (10μg/ml), EGF (20 ng/ml), hydrocortisone (0.5μg/ml), and cholera toxin (100 ng/ml). Human umbilical vein endothelial cell (HUVEC) was purchased from Lifeline Cell Technology® (Walkersville, MD) and maintained in VascuLife Basal Medium Supplemented with SMC LifeFactors. All cells were cultured in humidified atmosphere with 5% CO_2 at 37°C.

Plasmids

pCMX-mPPARγ1 was a gift from Dr. C. Glass. The cDNA of mouse PPARγ was amplified by PCR and subcloned into p3xFLAG CMV10 vector (Sigma) and pACT vector (Promega) to express 3xFLAG-tagged (FLAG-PPARγ) and VP16 fusion protein (PγCA), respectively. The coding region of 3xFLAG-PPARγ1 cDNA or PγCA cDNAs (5) was inserted into the MSCV-IRES-GFP vector at the *EcoRI* site (blunted) upstream of the IRES driving expression of GFP.

Subcutaneous Tumor Implantation

The NAFA cells derived from oncogenic MMTV-ErbB2 transgenic mice stably expressing PPARγ or PγCA were implanted by subcutaneous injection in the flank of female 6- to 8- week old FVB mice. Comparisons were made for 10–15 animals in each group between NAFA/GFP, NAFA/PPARγ, and NAFA/PγCA. The tumor growth rates were examined using serial caliper measurements. The tumor volume were calculated using the equation $(a^2 \times b)/2$ where "a" and "b" are length and width of the tumor, respectively. Tumors were weighed at the time of sacrifice. At the completion of the experiments, tumors were excised, weighed and statistical significance of differences in tumor volume were logarithm-transformed and analyzed using a linear mixed model. Separate slope and intercepts were computed for each group (GFP, PPARγ, PγCA), then compared across groups using a global test followed by pair-wise comparisons via linear contrasts. Data prior to Day 9 were ignored due to zeroes at Day 0 (inability to take logarithms) and an initial non-linearity/change in some of the animals growth patterns prior to Day 9. Thus, the intercept at Day 9 is interpretable as initiation of growth and the slope is interpretable as rate of growth. For the models, we report coefficients, confidence intervals of coefficients and 2-sided p-values. Analyses were completed in SAS v 9.1.3.

Western Blot

Conditioned cell culture medium were concentrated with Amicon Ultra 10K device (Millpore, MA) and separated by 10% SDS-PAGE and the proteins transferred to nitrocellulose membrane for Western blot as previously described (22). The following antibodies were used for Western blot: anti-Angptl4 (Invitrogen, CA), mouse M2 anti-FLAG antibody (Sigma).

Retrovirus Preparation and Infection

The MSCV-IRES-GFP retrovirus vector and the vector pSV-ψ-E-MLV that provides ecotropic packaging helper function and infection methods were described previously (23). Retroviruses were prepared by transient cotransfection of vector expressing PPARγ, PγCA and empty vector together with the helper viral vector into 293T cells, using calcium phosphate precipitation. The retroviral supernatants were harvested 48 h after transfection and filtered through a 0.45 μm filter. Mammary epithelial cells MCF10A, MCF10A/NeuT or NAFA were incubated with fresh retroviral supernatants in the presence of 8 μg/ml polybrene for 24 h, cultured for a further 48 hrs, and subjected to fluorescence-activated cell sorting (FACS) (FACStar Plus; BD Biosciences, San Jose, CA) to select for cells expressing GFP if infection efficiency was lower than expected (<80% GFP-positive cells). GFP-positive cells were used for subsequent analysis.

Nile Red Staining of Intracellular Lipid

Staining was carried out on living cells. When cells had grown to the desired confluence, dye was added to the cell culture at a final concentration of 100 ng/ml and incubated for a minimum of 5 minutes. Fluorescent and phase contrast imaging were collected using the 20x objective of an Olympus IX-70 Laser Confocal Scanning Microscope. Nile red exhibits red fluorescence.

Immunofluorescent Staining

Tumors from PPARγ, PγCA, and GFP vector control group were collected and fixed. The antibodies were directed to von Willebrad (vWF) (DAKO, Carpinteria, CA), c-Kit, CD133, and CD31 (BIOCARE Medical, Concord, CA) (24). Heat-induced epitope retrieval was performed on formalin-fixed and paraffin-embedded sections by incubating the sections in citrate buffer with 5% Tween 20 (pH 6.0) at 100°C for 20 minutes and allowed to cool for 20 minutes prior to staining. The sections were then incubated with 3% hydrogen peroxide diluted in 0.02 M PBS (pH 7.4) for 5 min at room temperature (RT), rinsed in 1x TBS for 15 min, and incubated with normal goat serum (PBS containing 10% normal goat serum and 2% bovine serum albumin) for 30 min at RT to block non-specific antibody binding. The slides were rinsed and incubated with primary antibody diluted to a concentration of 1:500 with PBS containing 2% goat serum overnight at 4°C. The slides were then rinsed as above and incubated with horseradish peroxidase (HRP)-conjugated secondary antibody according to the manufacturer's protocol (DAKO ENVISION, Carprinteria, CA). The signal was visualized using a Cyanine 3 (Cy-3) labeled Tyramide amplification system (Perkin Elmer Life Sciences, INC., Boston, MA). Sections were mounted in aqueous medium containing DAPI as a nuclear counterstain (Vector Labs). A negative control was performed to ensure the specificity of fluorescent immunostaining by replacing primary antibody with a normal rabbit IgG. Sections were examined with an Olympus BX 61 confocal microscope, and representative areas were photographed using 10X and 20X objective. The microvessel density (MVD) of the tumors were analyzed based on von Willebrand Factor (vWF) staining as previously described (25). Vessels were quantified at 200X using a linear encoded motorized XY stage (Prior, NJ). At least 20 fields were quantified in 4 different tumor sections. The number of capillary vessels per square millimeter of tumor tissue was quantified using 10X eye pieces equipped with 10 × 1 mm by 10 × 1 mm graticule and was expressed as a percentage of area of the grid. For control, 30 fields were analyzed in 4 different tumor samples. At least 40 fields were counted in 3 tumor sections for each experimental group, and significance was analyzed using the student's t-test. A difference of $p < 0.05$ was considered to be statistically significant. All analyses were done with SPSS 11.5 software. Data are expressed as mean ± SEM.

Microarray analysis

Microarray analysis was conducted as described (26). Total RNA was isolated from tumors using Trizol and used to probe Affymetrix 430 2.0 arrays (Affymetrix, Santa Clara, CA). RNA quality was determined by gel electrophoresis. Probe synthesis and hybridization were performed according to the manufacturer's manual. Three arrays were used for each condition. Analysis of the arrays was performed using the statistical package R statistics package and the limma library of the Bioconductor software package. Arrays were normalized using Robust Multiarray Analysis (RMA) and the genes were ranked using the log odds ratios for differential expression. Briefly, a linear model was constructed using a factorial design and differentially expressed genes were obtained from PγCA and PPARγ expressing tumors. Finally, the top ranked genes that are differentially expressed in a PγCA- dependent manner were determined based on their log-odds ratio. These genes were then subjected to hierarchical clustering with "complete" agglomeration and each cluster was further analyzed based upon known function of the genes contained in the cluster.

Migration Assay

Transwell migration assays were performed as described before (25). Briefly, 4×10^4 GFP-positive cells were seeded on 8 μm pore-sized transwell filter insert (Costar). After 16 hours incubation at 37°C and 5% CO_2, cells adherent to the upper surface of the filter were removed using a cotton applicator. Cells were fixed with 3.7% formaldehyde, stained with crystal violet,

and the numbers of cells on the bottom were counted. Data were from three experiments done in triplicate (mean ± SEM).

Results

PγCA Induces Lipid Formation in Normal and Oncogene-transformed Mammary Epithelial Cells

To examine the effect of the constitutively active PPARγ (PγCA) on human breast cancer cellular proliferation, immortal MCF10A cells were transduced with expression vectors encoding either PPARγ or PγCA. Cells were selected by GFP expression from the viral expression vector. MCF10A cells transduced with PPARγ were more polarized and less spread than the vector control cells (Fig. 1A). PγCA induced a similar less spread morphology. Multiple small oil droplets, which stained positively with Nile Red (Fig. 1A), were identified in both PPARγ and PγCA transduced cells. MCF10A cells transformed with an activating ErbB2 mutant, NeuT, adopt a spindle-shaped and more polarized morphology (Fig. 1B). Transduction with PPARγ reduced the polarized morphology of MCF10A/NeuT cells (Fig. 1B) accompanied by the formation of a small number of lipid droplets. PγCA also reduced the polarized fibroblastoid morphology of MCF10A/NeuT cells with a relatively greater abundance of Nile Red-positive Oil droplets (Fig. 1B). The accumulation of oil droplets is consistent with the known ability of liganded PPARγ to induce lipid metabolism in fibroblasts and enhanced transactivation of the PγCA in the absence of ligand.

PγCA Promotes Tumor Growth *in vivo*

The immortal and transformed MCF10A cells, grown in culture with matrix-rich basement membrane constituents, formed spherical structures in which the outermost layer forms polarized epithelium with the basal surface associating with surrounding basement member proteins and the apical surface pointing inward as previously shown (27). PγCA expression disorganized the polarized structure of MCF10A and MCF10A/NeuT cells (data not shown). The effect of PγCA on ErbB2-induced tumor was next examined *in vivo* in immune-competent animals (Fig. 2). ErbB2-expressing mammary tumor cells (NAFA) derived from MMTV-ErbB2 (FVB) transgenic mice were implanted into FVB animals. The size of PγCA-expressing tumors was greater than either wild-type PPARγ or GFP control group (Fig. 2A). Tumor volume was enhanced approximately 2-fold by PγCA compared to wild-type PPARγ (Fig. 2B). Supplemental Figure 1 (A–C) displays the individual animal growth profiles (dashed lines) as well as the group-specific linear growth models (solid lines). Supplemental Figure 1D displays the fitted growth models for all three groups. Table 1 provides the parameter estimates from each of these models in addition to information on statistical comparisons. PPARγ-expressing tumors demonstrated significantly lower initial growth rates than the GFP group (intercept difference=−0.66, p=0.01; 95% CI=−1.18, −0.14). PγCA-transduced tumors had significantly lower initial growth rates than GFP-expressing tumors (difference=−0.77, p=0.003; 95% CI= −1.27, −0.27). This finding is consistent with our observation that NAFA cells expressing PγCA had decreased proliferation rates compared to the control group (data not shown). The PPARγ-expressing tumor growth rates did not differ from GFP, whereas PγCA-expressing tumors had a significantly higher rate of growth than either GFP or PPARγ (slope=0.07, p<0.001; 95% CI=0.04, 0.10), (slope=0.06, p<0.001; 95% CI=0.03, 0.09). Collectively, these studies demonstrate PγCA promotes ErbB2-induced tumor growth in immune-competent animals.

PγCA Promotes Angiogenesis

Growth and formation of capillary blood vessels are essential steps required for sustained tumor growth and metastasis and contributes to cancer progression *in vivo*. To determine the mechanism(s) through which PγCA enhanced ErbB2-mediated tumor growth *in vivo*, we

analyzed blood vessels located in both the periphery and interior of tumors. Von Willebrand factor (vWF) is broadly accepted as a marker for endothelial cells. Immunofluorescent staining using anti-vWF antibody demonstrated increased blood vessel density in PγCA expressing tumors compared to GFP control tumors. Tumors expressing wild-type PPARγ alone did not affect vWF expression (Fig. 3A). Immunohistochemistry staining with an antibody against Platelet Endothelial Cell Adhesion Molecule-1 (PECAM-1, also known as CD31) (Fig. 3B) showed a similar result. Blood vessels in tumors derived from endothelial progenitor cells are characterized by CD133 and c-Kit (28,29). Increased expression levels of both CD133 and c-Kit were demonstrated in the PγCA expressing tumors, but not in GFP control or PPARγ expressing tumors (Fig. 3C). This finding suggests that circulating EPCs, released from the bone marrow may contribute to the increased vasculogenesis in ErbB2-induced tumors expressing active PPARγ.

Expression Profiling of PPARγ Target Genes in Mammary Tumors

In order to investigate the molecular mechanism(s) by which PγCA regulated angiogenesis/vasculogenesis, a genome-wide expression array analysis was conducted. Total RNA was prepared from extirpated tumors grown in immune-competent mice. Gene expression profiles were compared between the PPARγ and PγCA tumors (Fig. 4). Gene targets differentially regulated by PγCA convey functions in cell communication, angiogenesis, cell cycle, signal transduction, and cell differentiation. Genes regulated by PγCA in the angiogenesis pathway include Angiopoietin-like 4 (Angptl4), Fibroblast growth factor 9 (Fgf9), Fibroblast growth factor 1 (Fgf1), Adrenomedullin (Adm), Matrix metallopeptidase 12 (Mmp12), BCL2/adenovirus E1B 19kDa interacting protein 3 (Bnip3), Pleiotrophin (Ptn), Chemokine (C-X-C motif) ligand 2 (Cxcl2), and Vascular endothelial growth factor A (Vegfa) (Fig. 4B). We validated several genes including Angptl4, Fgf1, and Ptn by qRT-PCR on additional tumor samples (Fig. 4C). Angptl4 was cloned as a PPARγ target gene and initially termed as PGAR (PPARgamma angiopoietin related) and FIAF (fasting induced adipose factor) according to the nature of how this gene was discovered (30,31). We had previously shown that Angptl4 was up-regulated in primary culture of mammary epithelial cells transduced with PγCA (32). Angptl4 is a secreted protein, which belongs to the family of angiopoietin-like proteins. We further showed that Angptl4 secretion was increased in PγCA transduced NAFA cells compared to PPARγ and vector control (Fig. 4D, upper panel).

PγCA Promotes Endothelial Cell Migration through Induction of Secreted Factors

As PγCA induced the expression of genes governing angiogenesis, we hypothesized that secreted factors were involved. We examined the conditioned medium from PγCA expressing cells in endothelial cell migration assays. Transwell migration assays were conducted. Conditioned medium was collected from MCF10A/NeuT cells expressing GFP, PPARγ, or PγCA and applied to either the top or the lower chamber (Fig. 5A). Human umbilical vein endothelial cells (HUVECS) were seeded in the Boyden chamber and the cells migrating across the membrane were stained with crystal blue and counted (Fig. 5B). When conditioned medium from cells expressing PγCA were added to the bottom chamber, the number of migrating cells compared to GFP and PPARγ groups was significantly increased (Fig. 5B, left panel). When HUVECs were seeded in the conditioned medium in the top chamber, the number of cells migrating toward the serum-free medium (in the bottom chamber) were significantly reduced (Fig. 5B, right panel). These observations suggest that PγCA expression in breast cancer cells induces secreted factors that promote endothelial cell migration.

Angptl4 Mediates PγCA Induction of Angiogenesis

Angptl4 stimulates endothelial cell growth and tubule formation, which is required for neovascularization and adipose tissue expansion (33). Angptl4 functions to regulate

angiogenesis/vasculogenesis (33–35), which contributes to solid tumor growth (35). As PγCA induced Angptl4 expression and secretion, we determined the role of Angptl4 in PγCA-induced endothelial cell migration. To deplete Angptl4 proteins, the conditioned medium from MCF10A/NeuT/PγCA cell culture was incubated with an Angptl4 antibody conjugated to protein A agarose beads. Conditioned medium depleted of Angptl4 was assessed in HUVEC transwell migration assays. As we expected, more cells cultured in Angptl4-depleted medium trans-migrated to the bottom chamber compared to the IgG control (Fig. 5C), indicating Angptl4-containing medium is more favorable to endothelial cells. These studies suggest that PγCA induction of Angptl4 in breast cancer cells promotes endothelial cellular migration.

Discussion

The current studies demonstrated that the growth of ErbB2-induced mammary tumors implanted in immune-competent animals is promoted by an activated PPARγ (PγCA) in contrast with a cytostatic effect of PγCA on cancer cell proliferation in tissue culture. The role of PPARγ in tumorigenesis remains poorly understood in regards to growth inhibition effects in cultured cells and in NMU or NMBA-induced mammary tumorigenesis. Genetic removal of one allele of the PPARγ gene predisposes mice to gastric cancer (36). The tumor implantation analysis showed that early growth initiation by PPARγ and PγCA was significantly lower than the initial growth rate of mammary tumors expressing GFP. These findings are consistent with prior studies in which PPARγ ligands enhanced DMBA-induced rat mammary adenocarcinoma (8) and promoted colonic tumor growth in Apc^{Min} mice fed a high fat diet (17). Targeted expression of an activated PPARγ to the mammary gland also enhanced tumorigenesis induced by polyoma middle T antigen (21). It is not feasible to directly compare the effect of PPARγ ligands with a PPARγ mutant that mimics the ligand activated state as some PPARγ ligands may possess receptor-independent functions. However, collectively these studies suggest that activated PPARγ can enhance mammary tumor growth induced by either ErbB2 or polyoma middle T antigen. The molecular mechanisms by which PγCA enhanced mammary tumorigenesis were investigated using gene expression profiling and we identified the induction of a pro-angiogenic pathway. In a prior study with a similar PPARγ mutant, gene expression analysis identified induction of Wnt signaling (21). It was proposed that the tumor promoting effects of active PγCA in the mammary epithelium was due to enhanced Wnt signaling (21).

PPARγ inhibits angiogenesis *in vitro* (37). PPARγ is expressed in endothelial cells and PPARγ ligands, 15d-PGJ2 and TZD, inhibit tubular structure formation and proliferation of endothelial cell (HUVECs) in tissue culture (38). Consistent with our findings a pro-angiogenic effect of PPARγ ligands was reported (39,40). PPARγ ligands promote angiogenesis *via* induction of VEGF in cardiac myofibroblasts and human vascular smooth muscle cells, but inhibit VEGF-mediated blood vessel formation in a Chick chorioallantoic membrane (CAM) model (41) suggesting cell type specific effects. The current studies of breast cancer *in vivo* using genome-wide expression screening showed PγCA induced the pro-angiogenic genes VEGFa, Fgf1, Fgf4, and Angptl4. Angptl4 belongs to an angiopoietin-like protein family and is secreted by adipocytes, hepatocytes, the placenta, as well as cancer cells. Although the role of Angptl4 in angiogenesis is controversial, Angptl4 promotes angiogenesis in obesity (33–35) and contributes to solid tumor growth (35).

Our studies suggest that PγCA induces the number of endothelial progenitor cells (EPCs) within mammary tumors. Since PPARγ increases hematopoietic cell differentiation toward endothelial lineage (42), blood vessels in tumors may be derived from endothelial progenitor cells (EPCs). Downregulation of PPARδ in EPCs reduced prostacyclin biosynthesis and decreased capillary formation in nude mice *in vivo* (43). Activation of PPARγ or PPARδ promotes angiogenic progenitor cell differentiation toward endothelial cell lineage and

facilitates vasculogenesis by increasing the population of hematopoietic stem cells in bone marrow and EPCs in peripheral blood (42,44). Patients with coronary artery disease who received pioglitazone had an increased number of EPCs compared to the placebo group and rosiglitazone increased the number and migratory activity of EPCs in Type II diabetic patients (45,46).

The value of PPARγ as a potential target for the prevention and treatment of cancer using differentiation-based therapies revealed interesting preliminary observations (47), in which PPARγ ligand was used to treat human liposarcoma (48). However, a subsequent phase II trial failed to demonstrate an effect of rosiglitazone in liposarcoma (49) or in refractory breast cancer (50). The spread of obesity and increased prevalence of a sedentary lifestyle has substantially increased the incidence of type II diabetes. PPARγ agonists are increasingly used to enhance insulin sensitivity and improve glucose tolerance, and thereby reduce complications, including diabetic neuropathy, cardiovascular disease and retinopathy with blindness. As the current studies demonstrate that a ligand-activated PPARγ mutant promotes ErbB2 oncogene-induced tumorigenesis, further epidemiological studies are required in patients treated with PPARγ agonists for possible effects on tumor development.

Supplementary Material

Refer to Web version on PubMed Central for supplementary material.

Acknowledgments

This work was supported in part by awards from the Susan Komen Breast Cancer Foundation BCTR0504227 (C.W.), R01CA70896, R01CA75503, R01CA86072 (R.G.P.), and R01CA80250. Work conducted at the Kimmel Cancer Center was supported by the NIH Cancer Center Core grant (P30CA56036 (R.G.P.)). This project is funded in part by the Dr. Ralph and Marian C. Falk Medical Research Trust (R.G.P.), Pennsylvania Department of Health grant (to C.W., R.G.P.).

References

1. Rosen ED, Spiegelman BM. PPARγ: a Nuclear Regulator of Metabolism, Differentiation, and Cell Growth. J Biol Chem 2001;276:37731–4. [PubMed: 11459852]
2. Tontonoz P, Hu E, Spiegelman BM. Stimulation of adipogenesis in fibroblasts by PPARγ2, a lipid-activated transcription factor. Cell 1994;79:1147–56. [PubMed: 8001151]
3. Kim JB, Wright HM, Wright M, Spiegelman BM. ADD1/SREBP1 activates PPARgamma through the production of endogenous ligand. Proc Natl Acad Sci U S A 1998;95:4333–7. [PubMed: 9539737]
4. Yu S, Matsusue K, Kashireddy P, et al. Adipocyte-specific Gene Expression and Adipogenic Steatosis in the Mouse Liver Due to Peroxisome Proliferator-activated Receptor 1 (PPAR1) Overexpression. J Biol Chem 2003;278:498–505. [PubMed: 12401792]
5. Wang C, Pattabiraman N, Zhou JN, et al. Cyclin D1 repression of peroxisome proliferator-activated receptor gamma expression and transactivation. Mol Cell Biol 2003;23:6159–73. [PubMed: 12917338]
6. Brakenhielm E, Veitonmaki N, Cao R, et al. Adiponectin-induced antiangiogenesis and antitumor activity involve caspase-mediated endothelial cell apoptosis. Proc Natl Acad Sci U S A 2004;101:2476–81. [PubMed: 14983034]
7. Suh N, Wang Y, Williams CR, et al. A new ligand for the peroxisome proliferator-activated receptor-gamma (PPAR-gamma), GW7845, inhibits rat mammary carcinogenesis. Cancer Res 1999;59:5671–3. [PubMed: 10582681]
8. Pighetti GM, Novosad W, Nicholson C, et al. Therapeutic treatment of DMBA-induced mammary tumors with PPAR ligands. Anticancer Res 2001;21:825–9. [PubMed: 11396171]
9. Brockman JA, Gupta RA, Dubois RN. Activation of PPARgamma leads to inhibition of anchorage-independent growth of human colorectal cancer cells. Gastroenterology 1998;115:1049–55. [PubMed: 9797355]

10. Mueller E, Sarraf P, Tontonoz P, et al. Terminal differentiation of human breast cancer through PPAR gamma. Mol Cell 1998;1:465–70. [PubMed: 9660931]
11. Elstner E, Muller C, Koshizuka K, et al. Ligands for peroxisome proliferator-activated receptorγ and retinoic acid receptor inhibit growth and induce apoptosis of human breast cancer cells in vitro and in BNX mice. Proc Natl Acad Sci USA 1998;95:8806–11. [PubMed: 9671760]
12. Ricote M, Huang J, Fajas L, et al. Expression of the peroxisome proliferator-activated receptor gamma (PPARgamma) in human atherosclerosis and regulation in macrophages by colony stimulating factors and oxidized low density lipoprotein. Proc Natl Acad Sci USA 1998;95:7614–9. [PubMed: 9636198]
13. Sarraf P, Mueller E, Jones D, et al. Differentiation and reversal of malignant changes in colon cancer through PPARgamma. Nat Med 1998;4:1046–52. [PubMed: 9734398]
14. Sarraf P, Mueller E, Smith WM, et al. Loss-of-function mutations in PPAR gamma associated with human colon cancer. Mol Cell 1999;3:799–804. [PubMed: 10394368]
15. Kroll TG, Sarraf P, Pecciarini L, et al. PAX8-PPARgamma1 fusion oncogene in human thyroid carcinoma [corrected]. Science 2000;289:1357–60. [PubMed: 10958784]
16. Lefebvre AM, Chen I, Desreumaux P, et al. Activation of the peroxisome proliferator-activated receptor gamma promotes the development of colon tumors in C57BL/6J-APCMin/+ mice. Nat Med 1998;4:1053–7. [PubMed: 9734399]
17. Saez E, Tontonoz P, Nelson MC, et al. Activators of the nuclear receptor PPARgamma enhance colon polyp formation. Nat Med 1998;4:1058–61. [PubMed: 9734400]
18. Abe A, Kiriyama Y, Hirano M, et al. Troglitazone suppresses cell growth of KU812 cells independently of PPARgamma. Eur J Pharmacol 2002;436:7–13. [PubMed: 11834241]
19. Chawla A, Barak Y, Nagy L, Liao D, Tontonoz P, Evans RM. PPAR-gamma dependent and independent effects on macrophage-gene expression in lipid metabolism and inflammation. Nat Med 2001;7:48–52. [PubMed: 11135615]
20. Moore KJ, Rosen ED, Fitzgerald ML, et al. The role of PPAR-gamma in macrophage differentiation and cholesterol uptake. Nat Med 2001;7:41–7. [PubMed: 11135614]
21. Saez E, Rosenfeld J, Livolsi A, et al. PPAR gamma signaling exacerbates mammary gland tumor development. Genes Dev 2004;18:528–40. [PubMed: 15037548]
22. Lee RJ, Albanese C, Stenger RJ, et al. pp60(v-src) induction of cyclin D1 requires collaborative interactions between the extracellular signal-regulated kinase, p38, and Jun kinase pathways. A role for cAMP response element-binding protein and activating transcription factor-2 in pp60(v-src) signaling in breast cancer cells. J Biol Chem 1999;274:7341–50. [PubMed: 10066798]
23. Neumeister P, Pixley FJ, Xiong Y, et al. Cyclin D1 governs adhesion and motility of macrophages. Mol Biol Cell 2003;14:2005–15. [PubMed: 12802071]
24. Chizea J, Dailey VK, Williams E, Johnson MD, Pestell RG, Ojeifo JO. Endothelial progenitor cells significantly contribute to vasculatures in human and mouse breast tumors. Open Hematol J 2008;2:30–62.
25. Ju X, Katiyar S, Wang C, et al. Akt1 governs breast cancer progression in vivo. Proc Natl Acad Sci U S A 2007;104:7438–43. [PubMed: 17460049]
26. Sakamaki T, Casimiro MC, Ju X, et al. Cyclin D1 determines mitochondrial function in vivo. Mol Cell Biol 2006;26:5449–69. [PubMed: 16809779]
27. Liu M, Ju X, Willmarth NE, et al. Nuclear factor-kappaB enhances ErbB2-induced mammary tumorigenesis and neoangiogenesis in vivo. Am J Pathol 2009;174:1910–20. [PubMed: 19349372]
28. Gao D, Nolan DJ, Mellick AS, Bambino K, McDonnell K, Mittal V. Endothelial progenitor cells control the angiogenic switch in mouse lung metastasis. Science 2008;319:195–8. [PubMed: 18187653]
29. Hilbe W, Dirnhofer S, Oberwasserlechner F, et al. CD133 positive endothelial progenitor cells contribute to the tumour vasculature in non-small cell lung cancer. J Clin Pathol 2004;57:965–9. [PubMed: 15333659]
30. Kersten S, Wahli W. Peroxisome proliferator activated receptor agonists. Exs 2000;89:141–51. [PubMed: 10997287]

31. Yoon JC, Chickering TW, Rosen ED, et al. Peroxisome proliferator-activated receptor gamma target gene encoding a novel angiopoietin-related protein associated with adipose differentiation. Mol Cell Biol 2000;20:5343–9. [PubMed: 10866690]
32. Zhou J, Zhang W, Liang B, et al. PPARgamma activation induces autophagy in breast cancer cells. Int J Biochem Cell Biol. 2009
33. Gealekman O, Burkart A, Chouinard M, Nicoloro SM, Straubhaar J, Corvera S. Enhanced angiogenesis in obesity and in response to PPARgamma activators through adipocyte VEGF and ANGPTL4 production. Am J Physiol Endocrinol Metab 2008;295:E1056–64. [PubMed: 18728224]
34. Hermann LM, Pinkerton M, Jennings K, et al. Angiopoietin-like-4 is a potential angiogenic mediator in arthritis. Clin Immunol 2005;115:93–101. [PubMed: 15870027]
35. Le Jan S, Amy C, Cazes A, et al. Angiopoietin-like 4 is a proangiogenic factor produced during ischemia and in conventional renal cell carcinoma. Am J Pathol 2003;162:1521–8. [PubMed: 12707035]
36. Lu M, Kwan T, Yu C, et al. Peroxisome proliferator-activated receptor gamma agonists promote TRAIL-induced apoptosis by reducing survivin levels via cyclin D3 repression and cell cycle arrest. J Biol Chem 2005;280:6742–51. [PubMed: 15569667]
37. Giaginis C, Margeli A, Theocharis S. Peroxisome proliferator-activated receptor-gamma ligands as investigational modulators of angiogenesis. Expert Opin Investig Drugs 2007;16:1561–72.
38. Xin X, Yang S, Kowalski J, Gerritsen ME. Peroxisome proliferator-activated receptor gamma ligands are potent inhibitors of angiogenesis in vitro and in vivo. J Biol Chem 1999;274:9116–21. [PubMed: 10085162]
39. Yamakawa K, Hosoi M, Koyama H, et al. Peroxisome proliferator-activated receptor-gamma agonists increase vascular endothelial growth factor expression in human vascular smooth muscle cells. Biochem Biophys Res Commun 2000;271:571–4. [PubMed: 10814503]
40. Chintalgattu V, Harris GS, Akula SM, Katwa LC. PPAR-gamma agonists induce the expression of VEGF and its receptors in cultured cardiac myofibroblasts. Cardiovasc Res 2007;74:140–50. [PubMed: 17320065]
41. Aljada A, O'Connor L, Fu YY, Mousa SA. PPAR gamma ligands, rosiglitazone and pioglitazone, inhibit bFGF- and VEGF-mediated angiogenesis. Angiogenesis 2008;11:361–7. [PubMed: 18810647]
42. Wang CH, Ciliberti N, Li SH, et al. Rosiglitazone facilitates angiogenic progenitor cell differentiation toward endothelial lineage: a new paradigm in glitazone pleiotropy. Circulation 2004;109:1392–400. [PubMed: 14993120]
43. He T, Lu T, d'Uscio LV, Lam CF, Lee HC, Katusic ZS. Angiogenic function of prostacyclin biosynthesis in human endothelial progenitor cells. Circ Res 2008;103:80–8. [PubMed: 18511850]
44. Han JK, Lee HS, Yang HM, et al. Peroxisome proliferator-activated receptor-delta agonist enhances vasculogenesis by regulating endothelial progenitor cells through genomic and nongenomic activations of the phosphatidylinositol 3-kinase/Akt pathway. Circulation 2008;118:1021–33. [PubMed: 18711014]
45. Pistrosch F, Herbrig K, Oelschlaegel U, et al. PPARgamma-agonist rosiglitazone increases number and migratory activity of cultured endothelial progenitor cells. Atherosclerosis 2005;183:163–7. [PubMed: 15907852]
46. Sorrentino SA, Bahlmann FH, Besler C, et al. Oxidant stress impairs in vivo reendothelialization capacity of endothelial progenitor cells from patients with type 2 diabetes mellitus: restoration by the peroxisome proliferator-activated receptor-gamma agonist rosiglitazone. Circulation 2007;116:163–73. [PubMed: 17592079]
47. Sporn MB, Suh N, Mangelsdorf DJ. Prospects for prevention and treatment of cancer with selective PPARgamma modulators (SPARMs). Trends Mol Med 2001;7:395–400. [PubMed: 11530334]
48. Demetri GD, Fletcher CD, Mueller E, et al. Induction of solid tumor differentiation by the peroxisome proliferator-activated receptor-gamma ligand troglitazone in patients with liposarcoma. Proc Natl Acad Sci U S A 1999;96:3951–6. [PubMed: 10097144]
49. Debrock G, Vanhentenrijk V, Sciot R, Debiec-Rychter M, Oyen R, Van Oosterom A. A phase II trial with rosiglitazone in liposarcoma patients. Br J Cancer 2003;89:1409–12. [PubMed: 14562008]

50. Burstein HJ, Demetri GD, Mueller E, Sarraf P, Spiegelman BM, Winer EP. Use of the peroxisome proliferator-activated receptor (PPAR) gamma ligand troglitazone as treatment for refractory breast cancer: a phase II study. Breast Cancer Res Treat 2003;79:391–7. [PubMed: 12846423]

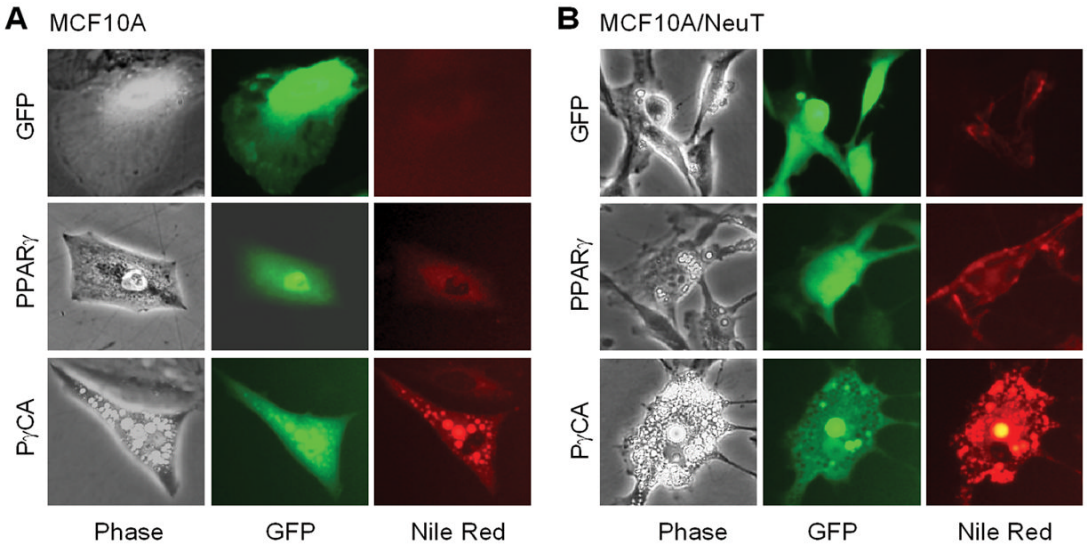

Figure 1. PγCA induces lipid formation of MECs cells transformed by ErbB2 oncogene

MCF10A or MCF10A/NeuT cells were infected with retroviral vector expressing GFP, PPARγ, and PγCA. 48 hr post-infection, cells were stained with Nile Red (100 ng/ml). Images were taken under a florescent microscope. GFP-positive cells were analyzed for accumulation of oil droplets within the cells as shown by Nile Red staining.

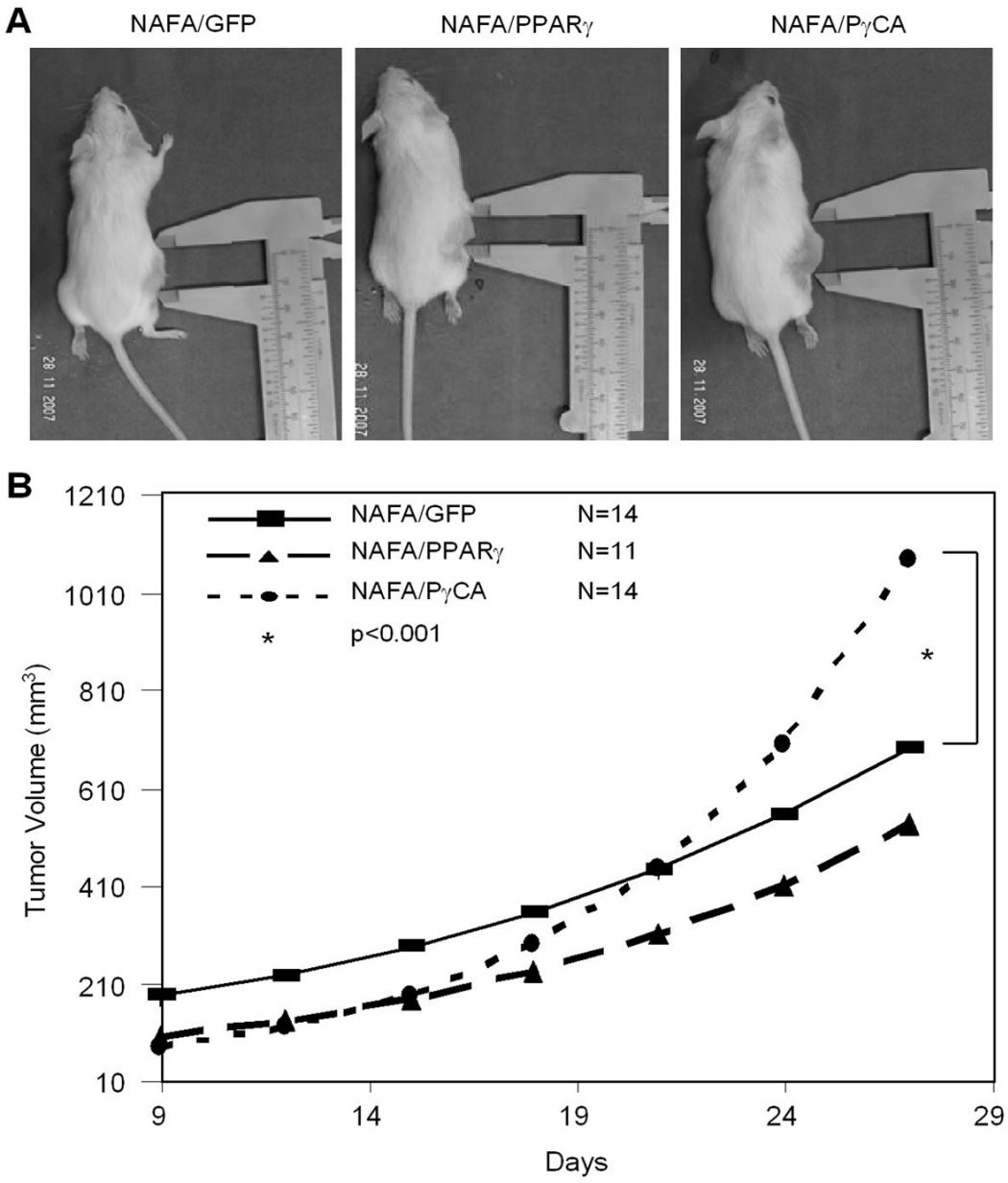

Figure 2. PγCA promotes tumor growth *in vivo*

A). NAFA cells transduced with MSCV-IRES-GFP vector encoding either PPARγ, PγCA, or empty vector were implanted into FVB by injecting 2×10^6 cells subcutaneously. Tumor growth was measured every three days by digital caliper and tumor volume was calculated. B). Tumor volumes were logarithm-transformed and analyzed using a linear mixed model. Separate slope and intercepts were computed for each group (GFP, PPARγ, and PγCA), then compared across groups using a global test followed by pair-wise comparisons via linear contrasts. Analyses were completed in SAS v 9.1.3, and detailed analysis can be found in Table 1 and Supplemental Figure 1.

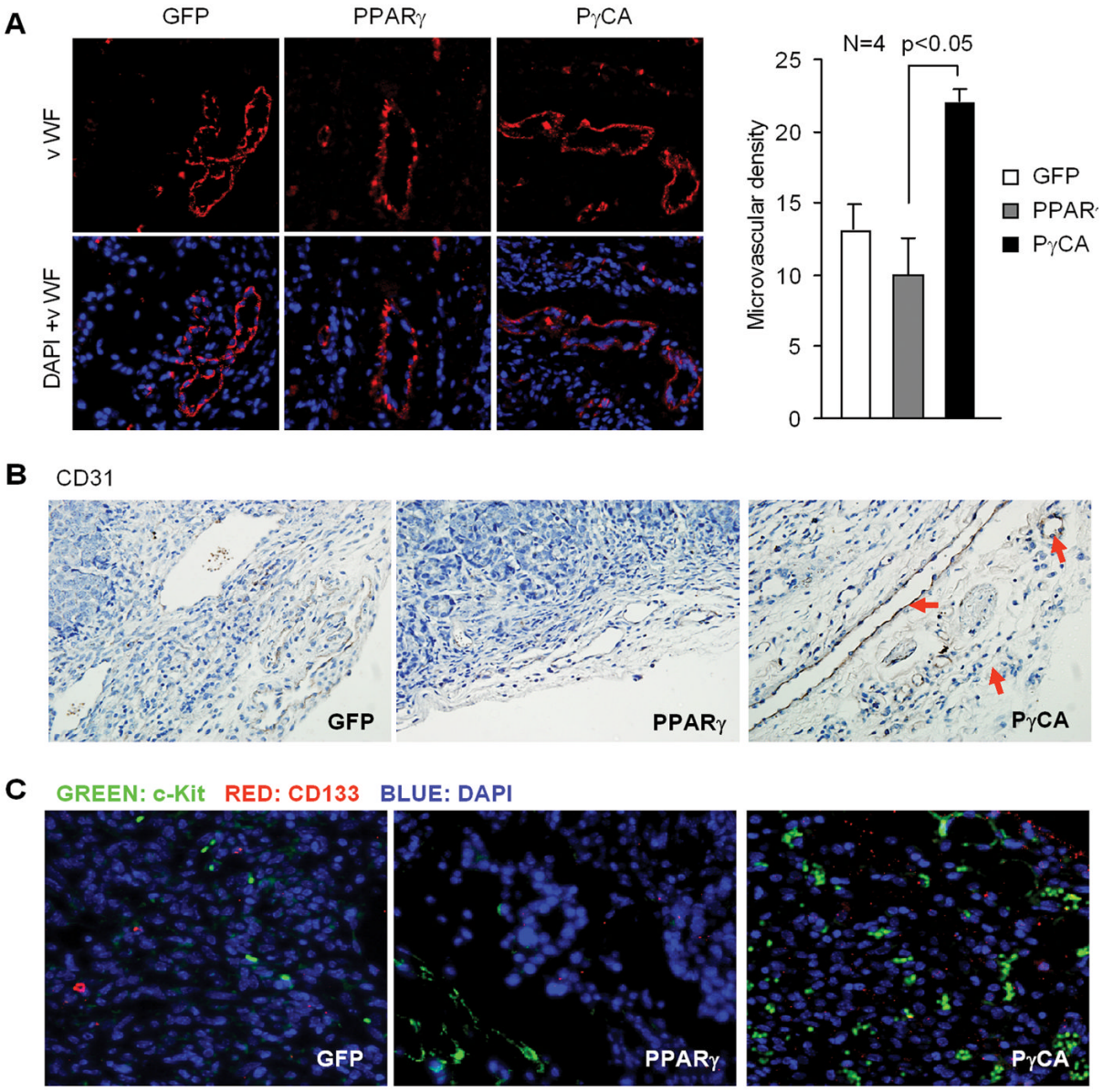

Figure 3. PγCA induces mammary tumor angiogenesis

A). Immunostaining was conducted using antibodies against vWF for microvessel formation. Microvessel density (MVD) was quantitated showing increased microvessel formation in PγCA group (22±1.5) compared to GFP control or PPARγ groups. B). Immunostaining was conducted in tumor samples to detect the expression levels of platelet endothelial cell adhesion molecule-1 (CD31) and CD133 (C).

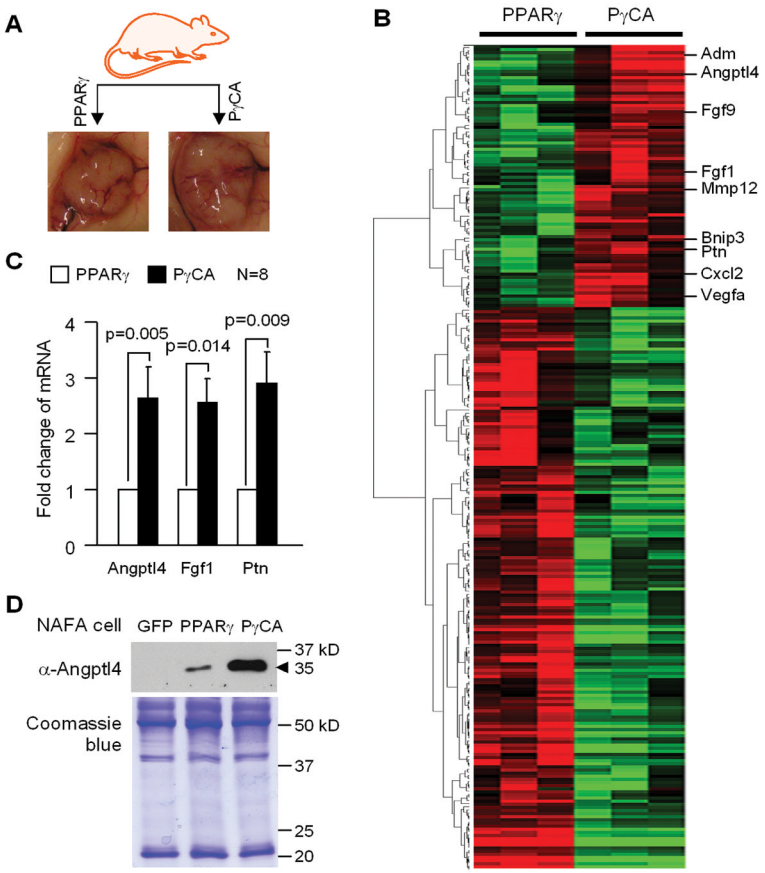

Figure 4. Gene expression profiling of tumors

A) Tumors from PPARγ and PγCA groups were collected when the tumor implantation experiment completed. Total RNA prepared from fresh tumors was used for gene profiling using Affymetrix gene expression array. B) Heatmap was generated based on the genes differentially regulated by PγCA and PPARγ. C) qRT-PCR was performed to quantitatively measure the mRNA abundance of Angptl4, Fgf1 and Ptn. D) 10 ml of conditioned medium were concentrated to 100 μl. 50 μl was used for Western blot to determine the abundance of the secreted form of Angptl4 (upper panel). 10 μl of medium were separated on 10% SDS-PAGE gel followed by staining the gel with Coomassie blue to show the equal loading (low panel).

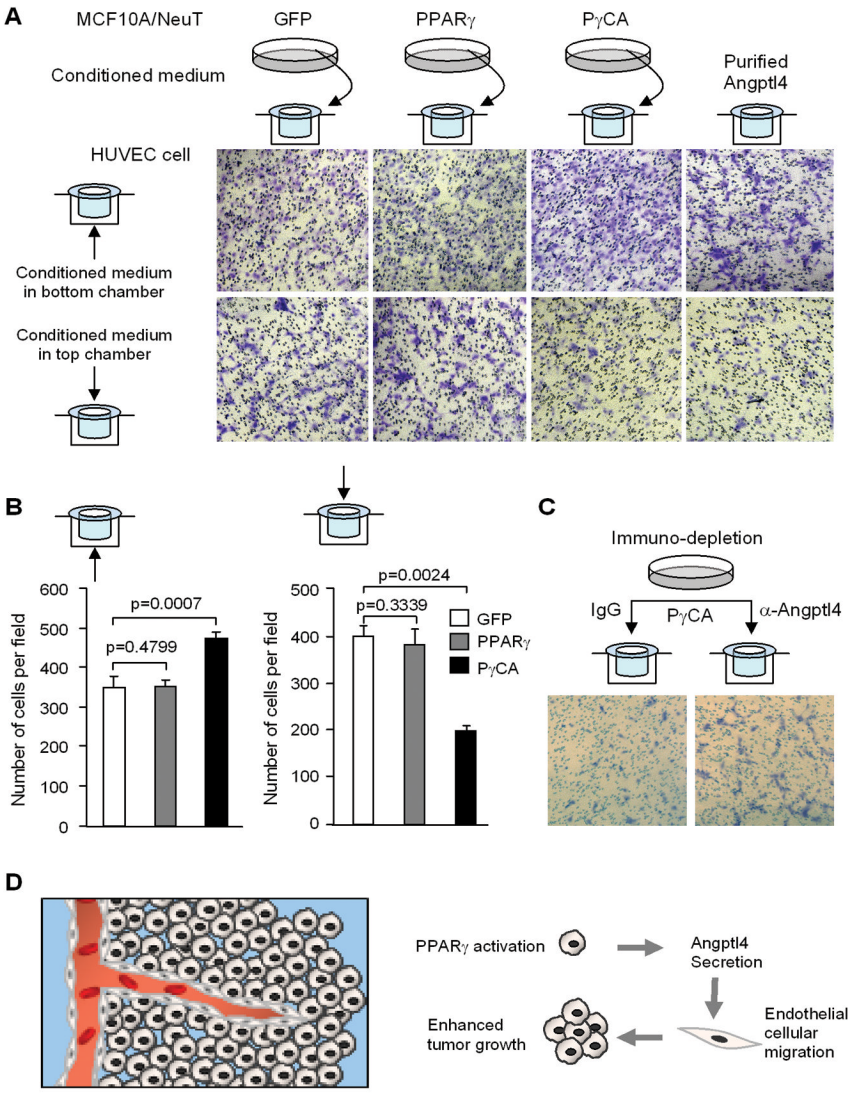

Figure 5. PγCA induction of pro-angiogenic factor Angptl4 in tumor cells is required for HUVEC cell migration

Transmigration assay was performed with HUVECs. Conditioned medium was collected from MCF10A/ErbB2 cells transduced PPARγ, PγCA, GFP control. Conditioned medium was applied to either bottom or top chamber of Transwell devise as illustrated. Transmigrating cells were visualized by staining with crystal violet (A) and quantified (B). Purified Angptl4 was included as positive control. C) Conditioned medium was pre-treated with antibody to deplete Angptl4. Conditioned medium was applied to the top chamber of Transwell device. Transmigrating cells were visualized by staining with crystal violet. D). Schematic representation of active PPARγ promotion of tumor growth through enhanced angiogenesis by inducing Angptl4 production.

Table 1

Linear mixed model coefficients for growth models.

Group	Coefficient	Std Error	t -value	p[⊥]	Difference vs GFP	95% Confidence Interval (CI)	p[#]	Difference vs PPARγ	95% Confidence Interval (CI)	p[#]
Intercept (Growth initiation)										
GFP	5.22	0.19	28.02	<0.001	--	--	--	--	--	--
PPARγ	4.55	0.18	13.99	<0.001	−0.66	−1.18, −0.14	**0.01**	--	--	--
PγCA	4.45	0.16	12.67	<0.001	−0.77	−1.27, −0.27	**0.003**	−0.11	−1.48, −0.01	0.61
Slope (Rate of Growth)										
GFP	0.08	0.01	6.68	<0.001	--	--	--	--	--	--
PPARγ	0.09	0.01	7.51	<0.001	0.01	−0.02, 0.06	0.26	--	--	--
PγCA	0.15	0.01	14.11	<0.001	0.07	0.04, 0.10	**<0.001**	0.06	0.03, 0.09	**<0.001**

[⊥]p-value is based on testing significance of individual coefficient using t-test

[#]p-value is based on testing significance of comparing coefficients across 2 groups by t-test